Published OnlineFirst August 7, 2008; DOI: 10.1158/1535-7163.MCT-08-0430

Human colorectal tumors and metastases express Gb_3 and can be targeted by an intestinal pathogen-based delivery tool

Thomas Falguières,[1] Matthias Maak,[2] Claus von Weyhern,[3] Marianne Sarr,[1] Xavier Sastre,[4] Marie-France Poupon,[5] Sylvie Robine,[1] Ludger Johannes,[1] and Klaus-Peter Janssen[2]

[1]Centre de Recherche, Institut Curie, CNRS UMR144, Paris, France; [2]Department of Surgery, Klinikum rechts der Isar, Technische Universität München, Germany; [3]Institut für Allgemeine Pathologie und Pathologische Anatomie, Technische Universität München, Germany; [4]Service d'Anatomo-pathologie, Institut Curie, Paris, France; and [5]Unité 612 INSERM/Institut Curie, Paris, France

Abstract

The targeting of solid tumors requires delivery tools that resist intracellular and extracellular inactivation, and that are taken up specifically by tumor cells. We have shown previously that the recombinant nontoxic B-subunit of Shiga toxin (STxB) can serve as a delivery tool to target digestive tumors in animal models. The aim of this study was to expand these experiments to human colorectal cancer. Tissue samples of normal colon, benign adenomas, colorectal carcinomas, and liver metastases from 111 patients were obtained for the quantification of the expression of the cellular STxB receptor, the glycosphingolipid globotriaosyl ceramide (Gb_3 or CD77). We found that compared with normal tissue, the expression of Gb_3 was strongly increased in colorectal adenocarcinomas and their metastases, but not in benign adenomas. Short-term primary cultures were prepared from samples of 43 patients, and STxB uptake was studied by immunofluorescence microscopy. Of a given tumor sample, on average, 80% of the cells could visibly bind STxB, and upon incubation at 37°C, STxB was transported to the Golgi apparatus, following the retrograde route. This STxB-specific intracellular targeting allows the molecule to avoid recycling and degradation, and STxB could consequently be detected on tumor cells even 5 days after initial uptake. In conclusion, the targeting properties of STxB could be diverted for the delivery of contrast agents to human colorectal tumors and their metastases, whose early detection and specific targeting remains one of the principal challenges in oncology. [Mol Cancer Ther 2008;7(8):2498–508]

Introduction

Cancers of the colon and rectum (CRC) are the second leading cause of cancer-related mortality in North America, Europe, and Australia. The aggressiveness of the disease is directly correlated with the ability of the primary tumor to invade distant organs, most frequently the liver, and the 5-year survival of patients with distant metastasis present at the time of diagnosis is <10% (1). Therefore, specific targeting of primary tumors and distant metastases for diagnostic and therapeutic purposes remains one of the principal challenges in oncology, and requires the identification of molecular targets that are specifically expressed on tumor cells. Over the last years, several groups have reported that the glycosphingolipid globotriaosyl ceramide (Gb_3 or CD77), like other glycosphingolipids (2, 3), is expressed in human malignancies. Gb_3 expression has been shown in Burkitt's and centrofollicular lymphomas (4–7), in a wide range of solid tumors such as breast and ovarian carcinomas (8, 9), and in testicular seminomas (10). Moreover, it was recently reported that Gb_3 expression in human colorectal cancer correlates with invasiveness and the ability to form metastasis (11). Importantly, normal human intestinal epithelia do not express Gb_3, nor do they bind Shiga toxin (12–15). Thus, Gb_3 expression by human digestive cancers may be exploited for tumor delivery purposes using natural Gb_3 ligands, such as Shiga toxin from *Shigella dysenteriae* and the highly related verotoxins from enterohemorrhagic *Escherichia coli* strains (16).

These enteropathogenic toxins have naturally evolved to resist digestive enzymes and drastic pH changes in the intestinal lumen, and are able to cross the intestinal barrier to spread in the organism (17). These properties make them excellent candidates as molecular targeting devices of digestive tumors. Shiga toxin and verotoxins are composed of two subunits, the catalytic A-subunit that inhibits protein biosynthesis by modifying rRNA, and the nontoxic,

Received 8/29/07; revised 5/2/08; accepted 5/22/08.

Grant support: The French Ministry of Research (ACI Biologie du Développement et Physiologie Intégrative), Fondation de France, Association pour la Recherche sur le Cancer (nos. 3105, 4803, and 5177), Cancéropôle Ile-de-France, and Institut Curie (PIC Vectorisation; L. Johannes); a fellowship from Ligue Nationale contre le Cancer (T. Falguières); and the Deutsche Forschungsgemeinschaft and Kommission fuer Klinische Forschung (K.P. Janssen).

The costs of publication of this article were defrayed in part by the payment of page charges. This article must therefore be hereby marked *advertisement* in accordance with 18 U.S.C. Section 1734 solely to indicate this fact.

Note: T. Falguières and M. Maak contributed equally to this work.

Current address for T. Falguières: Department of Biochemistry, University of Geneva-Sciences II, Geneva, Switzerland.

Principal investigators: L. Johannes and K.P. Janssen.

Requests for reprints: Klaus-Peter Janssen, Department of Surgery, Klinikum rechts der Isar, Technische Universität München, Ismaninger Str. 22, 81675 Munich, Germany. Phone: 49-89-4140-2066; Fax: 49-89-4140-6031. E-mail: klaus-peter.janssen@lrz.tum.de

doi:10.1158/1535-7163.MCT-08-0430

Published OnlineFirst August 7, 2008; DOI: 10.1158/1535-7163.MCT-08-0430

noncatalytic homopentameric B-subunit (STxB). The latter is responsible for cellular targeting and intracellular transport of the holotoxin and can bind to up to 10 to 15 Gb_3 molecules (18). This clustering leads to the association of STxB/Gb_3 complexes with membrane microdomains (19), an important event for its intracellular trafficking (11, 20). In toxin-sensitive cells, Shiga toxin and the nontoxic STxB are targeted by retrograde transport from the plasma membrane to the endoplasmic reticulum via early endosomes and the Golgi apparatus (21, 22; for a review, see ref. 23). The catalytic A-subunit of Shiga toxin is transferred to the cytosol, using the cellular retrotranslocation machinery, whereas STxB remains in the endoplasmic reticulum/Golgi membrane system (24). Therefore, retrograde transport permits STxB to avoid degradation in lysosomes and recycling to the plasma membrane.

The stable association of STxB with cells might be a useful property for diagnostic or therapeutic delivery strategies. Another advantage of this system is that STxB can be manipulated without altering the affinity and specificity of its interaction with Gb_3 on target cells (25). Moreover, STxB is a little immunogenic protein with MHC dependence (26). In a study of 30 patients with Shiga-like toxin–induced hemolytic and uremic syndromes, no antibodies to VT1 or VT2 could be detected (VT, verotoxin; note that VT1, or Shiga-like toxin 1, is essentially the same protein as Shiga toxin; ref. 27). Furthermore, Ludwig and colleagues reported that only 5% of patients with hemolytic and uremic syndromes, and only 1.8% of healthy subjects, had antibodies to Shiga-like toxin 1 (28). In another study, 6 out of 21 patients with diarrhea induced by *S. dysenteriae* had antibodies to Shiga holotoxin, but none to STxB-derived peptides (29). Our own preclinical data on mouse models for CRC indicate that repeated uptake of STxB by the oral or intravenous route is well tolerated and does not cause adverse side effects (30).

In the present study, we expanded our previously published preclinical investigations (30) to human tumors. Instead of using established tumor cell lines that have been cultured for long periods of time, potentially leading to the acquisition of multiple genetic aberrations, we decided to study primary cultures of human tumor cells of the colon and rectum. Our results show that colorectal tumors express Gb_3, that primary tumor cells in culture clearly accumulate STxB via the retrograde route, and that STxB does not induce apoptosis in these cells. Furthermore, Gb_3 expression was observable in distant liver metastasis, but not in adenomas or normal tissue. Correspondingly, primary cells obtained from adenomas did not display STxB uptake. We conclude that the naturally evolved properties of STxB can be diverted for tumor delivery, with potential applications in tumor imaging and tumor therapy.

Materials and Methods

Patient Collective

Tissue samples were obtained from 111 patients admitted to the Surgical Department, Klinikum rechts der Isar, with the diagnosis of colorectal carcinoma. Mean age was 65.9 years (range, 23–92). Informed, written consent of all patients regarding the tissue samples was obtained previously. Median follow-up after surgery was 23 months. Three patients died due to unrelated causes, 19 died due to cancer progress or disease recurrence (local recurrence $n = 2$, lymph node recurrence $n = 1$, and metachronous distant metastases $n = 12$). Tumors were classified according to the International Union Against Cancer (UICC) for tumor localization, tumor grade, and staging, as summarized in Table 1. Histology-guided sample selection was done to identify a tumor content of >70%. In addition, five tumor samples from the small intestine were tested (two malignant lymphomas, one epidermoid carcinoma, one leiomyosarcoma, and one carcinoid tumor of neuroendocrine origin). All samples were snap-frozen in liquid nitrogen and stored in −80°C until use.

Reagents and Antibodies

Antibodies and reagents used were anti–caspase-3 (Cell Signaling Technology), anti-cytokeratin 20 (Dako), anti-golgin p97 (Molecular Probes), anti-STxB (24), anti-CD11c, anti-CD11b (BD Biosciences PharMingen), anti–Ep-CAM (BerEP4, Dianova), TRITC-phalloidin, 4′,6-diamidino-2-phenylindole, staurosporine (Sigma-Aldrich), anti-CD77

Table 1. Clinical data

Patients	$n = 111$	
Female	49	44.1%
Male	62	55.9%
Location of tumor	$n = 97$	
Cecum	14	14.4%
Ascending colon	23	23.7%
Hepatic flexure	2	2.1%
Transverse colon	7	7.2%
Splenic flexure	2	2.1%
Descending colon	7	7.2%
Sigmoid colon	21	21.6%
Rectosigmoid	4	4.1%
Rectum	3	3.1%
Metastasis of the liver	14	14.4%
International Union Against Cancer staging	$n = 83$	
I	16	19.3%
II	25	30.1%
III	27	32.5%
IV	15	18.1%
Grade	$n = 83$	
G1	1	1.2%
G2	48	57.8%
G3	34	41.0%
Tumor invasion	$n = 83$	
pT_2	20	24.1%
pT_3	45	54.2%
pT_4	18	21.7%
Lymph node status	$n = 83$	
pN_0	44	53.0%
pN+	39	47.0%
Lymphatic invasion	$n = 83$	
Absent	66	79.5%
Present	17	20.5%

Published OnlineFirst August 7, 2008; DOI: 10.1158/1535-7163.MCT-08-0430

antibody (rat IgM, clone 38-13; Coulter), and anti-vimentin (Santa Cruz Biotechnology). Secondary antibodies coupled to fluorophores were purchased from Jackson ImmunoResearch. Cell culture reagents were purchased from Invitrogen.

Indirect Immunofluorescence

Immunostaining was done as described before (30). Briefly, after PFA fixation, the primary cultures on coverslips were permeabilized with 0.1% Triton X-100, blocked with PBS containing 2% bovine serum albumin, and primary antibodies in blocking buffer were added before counterstaining with secondary antibodies. STxB (which has 100% sequence identity with VT1B) was purified from bacteria as previously described (31). Covalent coupling of STxB to Cy3 (cyanine 3; Amersham Biosciences) fluorochrome (STxB-Cy3) was carried out according to the instructions of the supplier. For the staining of endogenous Gb_3, tissue cryosections were fixed with 3% paraformaldehyde at room temperature for 20 min and incubated with STxB-Cy3 for 30 min at a final concentration of 10 μg/mL in PBS containing 0.2% bovine serum albumin. For image acquisition, epifluorescence or confocal microscopes (Zeiss) were used. Images were processed using Adobe Photoshop Software. Cytochrome *c* cytosolic release was analyzed on primary colon tumor cells with the SelectFX kit (Molecular Probes), according to the instructions of the manufacturer. Adherent primary cultured cells were incubated with anti-Gb_3/CD77 antibody (50 μg/mL) and goat anti-rat IgM (10 μg/mL) in 1 mL of complete primary culture medium for 24 h at 37°C before fixation and further processing.

Quantification of Gb_3 Expression by TLC

Tumors were collected by an experienced pathologist, frozen in liquid nitrogen immediately after surgery, and stored at −80°C. Tissues were weighed and mechanically homogenized in 1 mL of water. Gb_3 expression was quantified after lipid extraction, STxB overlay, and immunodetection as previously described (20).

Establishment of Primary Cultures

Primary cell cultures were established from adenomas, colorectal carcinomas, and metastases of the liver essentially as described before (30). Briefly, fresh tumor biopsies were obtained by an experienced pathologist and, immediately after surgery, placed in tissue collection medium (DMEM supplemented with 2.5% heat-inactivated FCS, 1% penicillin/streptomycin, 1% gentamicin, 1% fungizone, and 1% glutamine) at 4°C. The tissue was then dissected with the help of a sterile blade, and subjected to enzymatic digestion with collagenase (0.2 mg/mL; Roche) and dispase (0.1 mg/mL, Roche) in digestion medium containing DMEM supplemented with 0.5% heat-inactivated FCS, antibiotics as above, 0.2 units/mL of insulin, and 10 ng/mL of epithelial growth factor. Enzymatic treatment was carried out for 2 to 3 h under constant shaking at 37°C. By differential centrifugation (400 rpm, 5 min, at room temperature), organoids were separated from debris and single cells. The pellet was resuspended in primary culture medium (DMEM supplemented with 20% heat-inactivated FCS, antibiotics as above, 0.2 units/mL insulin, and 10 ng/mL epithelial growth factor), plated on gelatin-coated glass coverslips, and incubated under standard growth conditions (5% CO_2 at 37°C). Medium was changed after 2 days, and STxB incubation was carried out without further trypsinization.

STxB Uptake Assays

STxB-Cy3 was added at a final concentration of 2.5 μg/mL. After various time points of incubation at 37°C, primary cells were fixed with 3% paraformaldehyde and analyzed by immunofluorescence. In 15 cultures, STxB-induced apoptosis was studied after incubation for 48, 72, or 120 h at 37°C with labeled or unlabeled STxB at either 0.5 or 2.5 μg/mL. As a positive control for apoptosis induction, cells were incubated with staurosporine, added to a final concentration of 1 μmol/L for 6 h prior to fixation. Apoptosis was quantified by immunofluorescence staining for cleaved caspase-3, and by evaluation of fragmented nuclear morphology after 4′,6-diamidino-2-phenylindole staining.

Preparation of Xenografts

Colon cancer samples were obtained from the Institut Gustave Roussy in accordance with protocols approved by the local ethics committee. Tumor material was placed in collecting medium (DMEM supplemented with 10 mmol/L HEPES, 1 mmol/L pyruvate sodium, 200 units/mL penicillin, 200 μg/mL streptomycin, 200 μg/mL gentamicin, 5 μg/mL ciprofloxacine, 20 μg/mL metronidazole, 25 μg/mL vancomycin, and 2.5 μg/mL fungizone), as described (32). Five-week-old Swiss *nu/nu* (nude) male mice were used as xenograft recipients; they were bred in the animal facilities of the Institut Curie and maintained in specified pathogen–free conditions. Their care and housing were in accordance with national and institutional guidelines under the supervision of an authorized investigator (M.F. Poupon). Subcutaneous tumor implantation procedures were done as described in detail elsewhere (32).

Results

Gb_3 Is Expressed in Human Colorectal Cancer and Liver Metastasis

Using lipid extraction and TLC, we have shown in a previous study that Gb_3 is expressed by intestinal tumors in genetically defined mouse models (30). In the present work, we have applied this method to human tissue samples. In a first series of experiments, human colorectal tumors from 33 patients were xenografted in nude mice and analyzed for Gb_3 expression. Approximately 20% of the tumors showed high expression levels (>30 ng Gb_3/mg tissue; Fig. 1A). Next, we analyzed a series of freshly resected tissue samples. Benign adenomas (n = 12) showed no deregulation of Gb_3 expression as compared with normal colon samples from 19 patients. Primary human colon carcinomas (n = 66) expressed, on average, 3-fold more Gb_3 as compared with normal tissue. This difference was highly significant (P = 0.002; Fig. 1B). The expression varied in

Published OnlineFirst August 7, 2008; DOI: 10.1158/1535-7163.MCT-08-0430

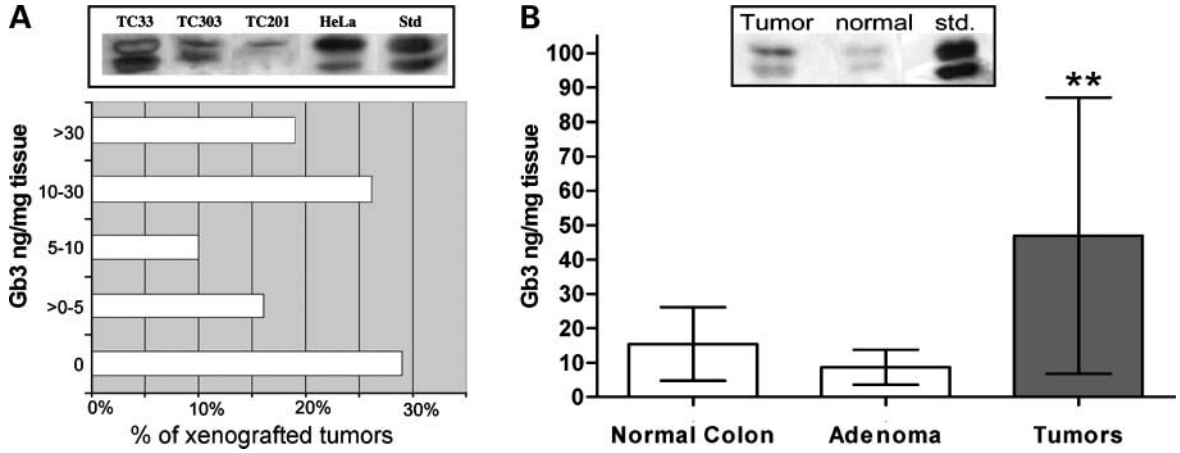

Figure 1. Gb_3 is overexpressed in primary or xenografted human CRC. Gb_3 levels were determined in duplicate. **A,** samples from 33 xenografted human CRC were grouped in categories according to Gb_3 expression. *Inset,* typical results from TLC. Extracts from HeLa cells were loaded as a positive control, next to the standard purified Gb_3, and three representative tumor xenograft samples with strong (*TC33*), intermediate (*TC303*), or weak (*TC201*) Gb_3 expression. Note that Gb_3 appears as a doublet. **B,** Gb_3 was quantified from normal colon (n = 19), adenomas (n = 12), and colorectal tumors (n = 66). *Columns,* mean; *bars,* SD. The difference in Gb_3 expression was highly significant between tumors and normal tissue (**, P = 0.002). *Inset,* typical result from chromatography.

individual tumor samples from 0.4-fold to 14-fold, compared with the average mean expression in normal colon. This distribution is likely due to the genetic heterogeneity of the human tumors. Moreover, the analysis was done on resected tumors, without prior microdissection. Even though histologic examination of control sections was used to ensure a tumor cell content of >70%, variable amounts of nontumor cells, such as stromal cells and infiltrating lymphocytes, were present in the samples. Thus, given tumor cell dilution, the actual expression of Gb_3 per tumor cells may be underestimated in our quantification experiments.

Gb_3 was readily overexpressed in early tumor stages (stage I according to International Union Against Cancer classification), and its expression was maintained throughout tumorigenesis and did not vary significantly during tumor progression (Fig. 2A). Of note, there was no significant difference in Gb_3 expression levels between tumors with (n = 31) or without (n = 35) metastasis. Gb_3 expression was not correlated to the age or sex of the patients, and there was no significant influence on the anatomic site of the tumor (colon or rectum, see Table 1). Corresponding samples of normal colon, primary tumor, and liver metastases were obtained from five individual patients, and analyzed for Gb_3 expression (Fig. 2B). In all cases, similar or even higher quantities of Gb_3 were detected in metastases, when compared with the primary tumor from the same patient. This is in good accordance with earlier findings (11). The expression levels were distinctly higher than in normal colon and normal liver parenchymal tissue (Fig. 2B). Lymph node metastases also expressed high levels of Gb_3 (n = 2; data not shown). These observations strongly suggest that metastases which originated from Gb_3-positive primary colorectal tumors maintained Gb_3 expression at distant sites.

The prognostic relevance of Gb_3 expression in primary tumors was also tested. There were no statistically significant differences in overall survival or recurrence-free survival between patients with low or high expression of Gb_3 in colorectal tumors. However, there was a trend towards increased mortality and bad prognosis in the group of patients with high Gb_3 expression levels in primary colorectal tumors (data not shown). Furthermore, we tested whether deregulated Gb_3 expression also occurred in less common lesions at other sites of the intestinal tract. One carcinoid tumor, one epidermoid carcinoma, one leiomyosarcoma, and two malignant lymphomas of the small intestine were analyzed for Gb_3 expression (Fig. 2C). In the first three cases, Gb_3 levels were similar to the mean levels observed on CRC, even though these tumor entities differ histologically from colorectal adenocarcinoma. Of note, Gb_3 was highly expressed in both malignant lymphomas samples, one of which was a follicular lymphoma, and the other one a high-grade lymphoma. Thus, despite the small sample size, it seems clear that several types of tumors from the small intestine express increased levels of Gb_3.

To determine the cellular origin of the increased Gb_3 levels, we detected endogenous Gb_3 on fixed cryosections. Normal colon epithelial tissue was found to be negative (Fig. 3A–C), similar with published observations by several other groups, and with the results we have obtained in murine tissue (30). Some occasional cells in normal tissue showed STxB labeling. These cells may correspond to the colonic myofibroblasts described by others (15), and this finding could explain, at least in part, that some Gb_3 was detected in normal intestinal tissue, as described above. Tumor cells arranged in glandular structures clearly showed STxB labeling (Fig. 3D–F). However, the intensity of STxB labeling in putative epithelial tumor cells was

Published OnlineFirst August 7, 2008; DOI: 10.1158/1535-7163.MCT-08-0430

heterogeneous within tumors (Fig. 3G–I). In contrast, stroma components were labeled throughout the tumor samples. It should be noted that the precise subcellular localization of Gb_3 might have been altered by the permeabilization step required for immunolabeling. In good agreement with these data on resected tissue samples, xenografts of human colorectal tumors also showed strong expression of Gb_3 in tumor cells arranged in glandular structures (Fig. 3J–L).

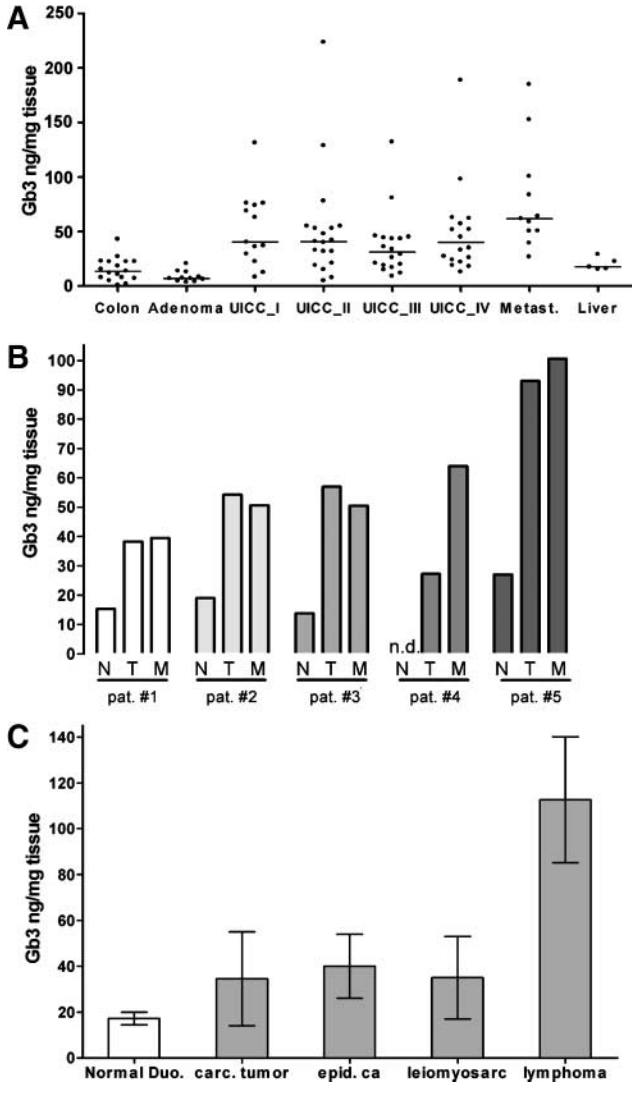

Figure 2. **A,** Gb_3 expression is increased starting with International Union Against Cancer (UICC) stage I carcinoma, and remains high throughout tumor progression. Each dot represents one patient; all samples were analyzed in duplicate. *Right,* Gb_3 expression in liver metastasis and in liver parenchyme. *Bars,* median. **B,** Gb_3 expression analysis on matched pairs of normal colon tissue (*N*), primary CRC (*T*), and liver metastasis (*M*) from five different patients, means of two quantifications. Normal tissue from patient no. 4 was not available for analysis. **C,** Gb_3 expression in small intestinal tumors. Normal tissue from normal duodenum of two patients as control; one carcinoid tumor, one epidermoid carcinoma, one leiomyosarcoma, and two malignant lymphoma samples were analyzed. *Columns,* mean of three extractions; *bars,* SD.

Uptake of STxB by Primary Tumor Cells

To investigate the potential use of STxB to target human colorectal tumors, we developed short-term primary cultures of tumor cells from the freshly resected samples described above (Fig. 1B). Primary cell cultures of 4 benign adenomas, 31 colonic carcinomas, 3 rectal carcinomas, and 6 metastases of the liver were established. Primary cultures of normal colonocytes could not be obtained, despite several attempts using freshly resected normal colon mucosa samples ($n = 6$). Even after long periods of incubation, only fibroblastic vimentin-positive cells could be identified on these cultures (data not shown).

The primary cultures were tested after 2 days for uptake of fluorescently labeled STxB. Cells derived from benign adenomas showed only low STxB uptake in this assay (Fig. 4A), in line with the low Gb_3 levels detected by extraction and overlay (Fig. 1B). In contrast, cells from primary tumors (Fig. 4B) or liver metastases (Fig. 4C) showed robust intracellular accumulation of STxB, as opposed to the negative controls without the addition of STxB (Fig. 4D). This indicates a clear correlation between Gb_3 expression and STxB uptake. Costaining with an antibody against cytokeratin 20 identified the STxB-positive cells as tumor cells of epithelial origin (Fig. 4E). These cells were also positive for the epithelial markers E-cadherin and Ep-CAM (data not shown). Interestingly, cells at the leading edge of epithelial islets from invasive tumors or liver metastases showed a pronounced STxB labeling in several cases (as seen in Fig. 4F). STxB was distributed in a perinuclear compartment in the tumor cells (Fig. 4G).

In addition to the islets of epithelially derived tumor cells, the primary cultures sometimes contained single interspersed cells that morphologically resembled fibroblasts. These cells indeed stained positive with an anti-vimentin antibody, a marker of mesenchymal cells, but they were negative for STxB uptake in most cases (*arrowheads*, Fig. 4H; *arrow,* a STxB-positive cell of putative epithelial origin that is negative for vimentin staining).

In cultures from 38 patients, the kinetics of intracellular STxB accumulation was analyzed by immunofluorescence. STxB-positive cells were identified by fluorescence microscopy after fixation at various time points of STxB uptake, and their numbers were related to the total number of cells present on the slides. After 1 hour of incubation at 37°C, $81 \pm 12\%$ of the tumor cells were positive for intracellular STxB, as analyzed from $n = 15$ tumors. In comparison, $35 \pm 21\%$ cells were positive in the group of $n = 4$ adenomas. When STxB was bound for 15 minutes to primary tumor cells on ice, cell surface staining was visible (Fig. 5A). After 15 minutes of incubation at 37°C, STxB clearly colocalized with the Golgi marker golgin p97 (Fig. 5B), and colocalization was even more pronounced after 60 minutes of incubation at 37°C (Fig. 5C). This indicates that STxB followed the retrograde route from the plasma membrane to the Golgi apparatus in the primary tumor cells, avoiding recycling or degradation. Three days after internalization, STxB was still detectable in punctate structures, but no obvious colocalization could be detected

Published OnlineFirst August 7, 2008; DOI: 10.1158/1535-7163.MCT-08-0430

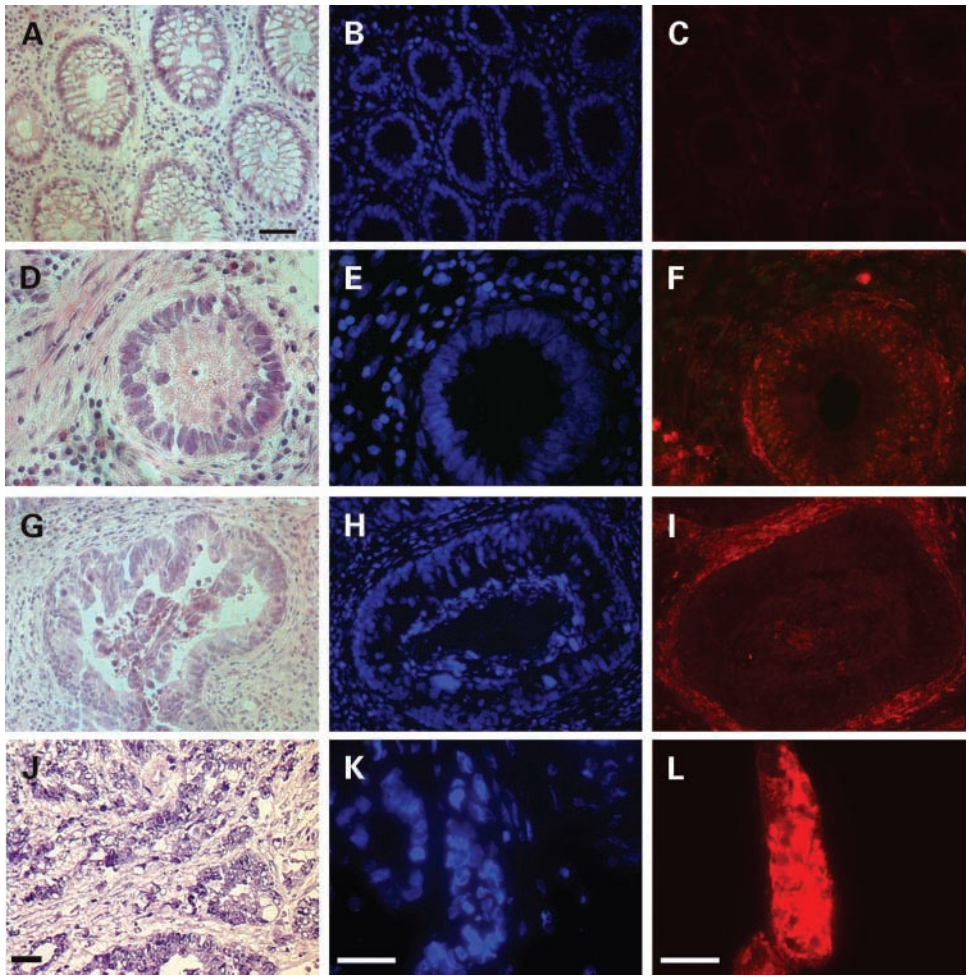

Figure 3. Immunocytochemical analysis of Gb_3 in primary and xenografted human CRC. Fluorescently labeled STxB was used on fixed tissue sections. The three different rows of images show standard H&E staining (*left*), which was carried out in parallel to the fluorescence staining on consecutive tissue sections; nuclear staining with 4′,6-diamidino-2-phenylindole (*middle*), and STxB overlay (*right*). **A** to **C,** normal tissue. Note the absence of STxB staining (**C**) on normal enterocytes and stromal tissue. **D** to **F,** CRC samples. STxB staining (**F**) is found on tumor enterocytes and in surrounding stromal tissue. Note that the precise subcellular localization of Gb_3 might have been altered by the permeabilization step required for immunolabeling. **G** to **I,** another region of the tumor sample analyzed in **D** to **F**. In this sample, the stromal tissue still strongly binds STxB (**I**), whereas tumor cells are only weakly labeled (*bar,* 50 μm). **J** to **L,** Gb_3 expression is maintained in xenografted human CRC. H&E staining showing an overview of the xenografted tumor in lower magnification (**J**). Nuclear staining (**K,** *blue*) and detection of Gb_3 with fluorescently labeled STxB (**L,** *red*).

with Golgi structures (Fig. 5D). The transport behavior in primary colorectal tumor cells observed here is similar to published results on human tumor cell lines (20). These data are also reminiscent of the ones obtained on primary cultures of murine digestive tumors (30). Quantification of the different intracellular localizations of Gb_3 from all experiments together revealed a rapid uptake into a perinuclear compartment within 1 hour of incubation, and the appearance of punctate, vesicular structures outside of the Golgi apparatus at later time points, first detectable after 48 hours (Fig. 5E).

We also studied if STxB induced apoptosis in the primary, nonpassaged tumor cells, as previously reported for established colorectal tumor cell lines (11). Both fluorescently labeled and nonmodified STxB were used for incubation at different concentrations with primary tumor cells from nine patients. Uptake was monitored by immunofluorescence microscopy, and apoptosis induction was analyzed by labeling with an antibody against cleaved caspase-3 (Fig. 5F), and by evaluation of nuclear morphology after Hoechst staining. In order to test for an induction of caspase-independent cell death, the cytosolic release of cytochrome *c* was analyzed (Supplementary Fig. S1).[6] Treatment with STxB did not induce caspase-3 cleavage (Fig. 5F) nor cytosolic release of cytochrome *c* (Supplementary Fig. S1A–F).[6] This shows that the STxB does not cause apoptosis in primary human colorectal cancer cells, neither by caspase-dependent nor by caspase-independent pathways.

Two independent pathways have been reported, at least in cells of lymphoid origin, that lead to apoptosis upon binding of either the holotoxin or a specific antibody to Gb_3/CD77 (33). Therefore, we have compared in parallel the effects of a specific anti-CD77 antibody with the uptake of STxB on primary colon cancer cells. Incubation with the specific antibody was carried out according to published protocols on cultures from three patients. No significant increase in the number of cells with cleaved caspase-3 (data not shown), or with cytosolic release of cytochrome *c*, was

[6] Supplementary material for this article is available at Molecular Cancer Therapeutics Online (http://mct.aacrjournals.org/).

Published OnlineFirst August 7, 2008; DOI: 10.1158/1535-7163.MCT-08-0430

observable in the anti-CD77 antibody–treated cells (Supplementary Fig. S1G–I).[6] Control experiments with staurosporine showed a reproducibly massive induction of apoptosis in all primary cells studied, as evidenced by cleavage of caspase-3 (Fig. 5F), or by cytosolic release of cytochrome *c* from mitochondria (Supplementary Fig. S1J–L).[6]

Discussion

In this study, we report a highly significant up-regulation of the glycosphingolipid Gb_3 in human colorectal cancer and liver metastases, as compared with normal colon tissue and benign lesions. In fact, on average, human colon carcinomas expressed 3-fold more Gb_3 as compared with

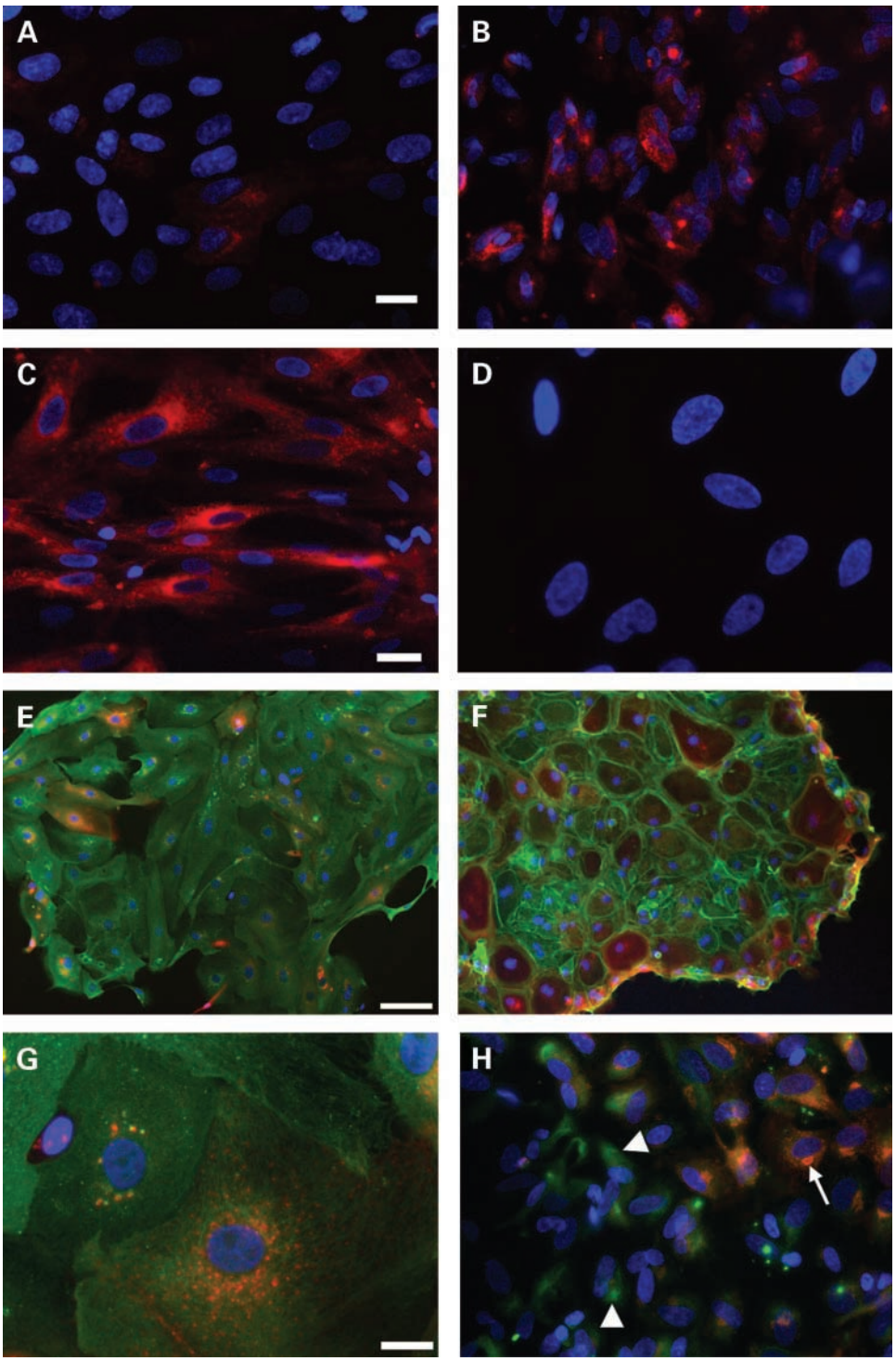

Figure 4. STxB uptake in primary cultures of colorectal tumors. Live cells were incubated with STxB at 0.5 μg/mL for 24 h, fixed, and processed for immunofluorescence; STxB (*red*) and nuclear (*blue*) staining. **A,** adenoma shows minor STxB uptake in contrast with primary colorectal adenocarcinoma (**B**) and liver metastasis (**C**). **D,** negative control without STxB. **E,** double-staining identifies the STxB-positive cells as tumor cells of epithelial origin. STxB (*red*) and cytokeratin-20 staining (*green*) in colon tumor cells. **F,** note that STxB (*red*) is enriched in cells at the periphery of the tumor cell islet; filamentous actin cytoskeleton (*green*). **G,** higher magnification shows perinuclear STxB (*red*) accumulation in a tumor cell marked by cytokeratin-20 (*green*). **H,** fibroblasts that are also present in the primary cultures were identified by vimentin staining (*green, arrowheads*). The vimentin-positive cells show no uptake of STxB (*red*), as opposed to adjacent tumor cells of epithelial origin (*arrow*).

Published OnlineFirst August 7, 2008; DOI: 10.1158/1535-7163.MCT-08-0430

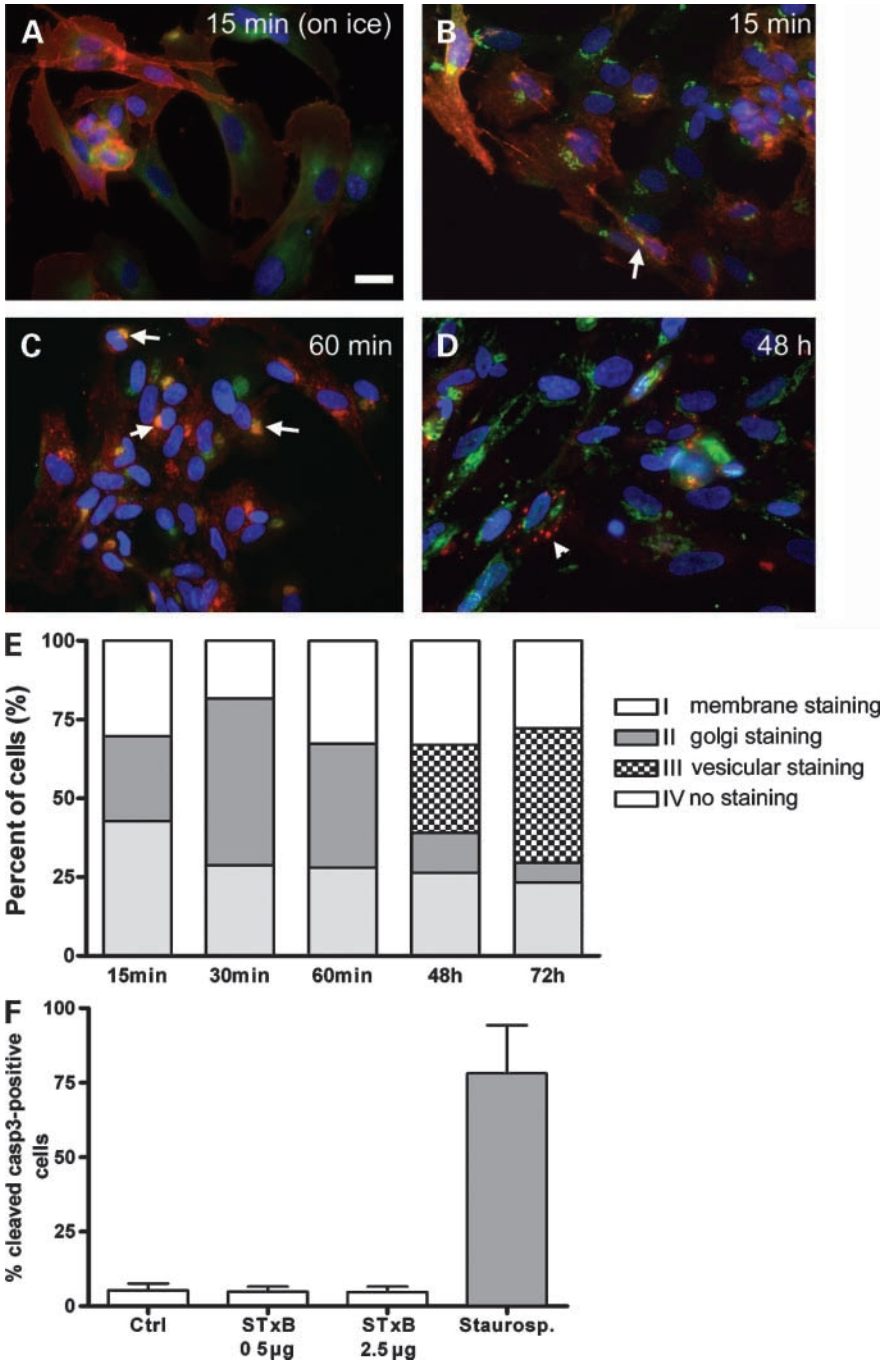

Figure 5. Analysis of intracellular uptake kinetics of STxB in primary colorectal tumor cells. **A** to **D,** STxB (*red*), costaining with anti-golgin p97 (*green*) and nuclear staining (*blue*). **A,** incubation with STxB was carried out on ice for 15 min. Note the plasma membrane staining for STxB. **B,** incubation with STxB at 37°C for 15 min, some colocalization with Golgi apparatus is already visible (*arrow*). **C,** incubation with STxB at 37°C for 60 min, prominent colocalization with Golgi (*arrows*). **D,** after 3 days in culture, STxB is still detectable in the primary tumor cells. Although, colocalization with the Golgi apparatus is not visible, the formation of intracellular vesicles is (*arrowhead*). **E,** cells from 15 independent experiments were analyzed, and the intracellular staining pattern of STxB was grouped into four different stages: (*I*) membrane staining, (*II*) colocalization with golgin p97, (*III*) vesicular staining, no colocalization with golgin p97, and (*IV*) no STxB staining visible. **F,** STxB uptake in primary tumor cells does not induce apoptosis. The number of cleaved caspase-3–positive cells was related to the number of total cells in 10 fields of view. Control incubation with the drug staurosporine leads to massive induction of apoptosis in all cases tested. Cells were treated with STxB at different concentrations (0.5 and 2.5 μg/mL) and analyzed at 48 h after incubation. *Columns,* mean; *bars,* SD (n = 8 patients).

normal tissue. Furthermore, a small sample number of rare human small intestinal tumors of different origin (lymphomas, epidermoid carcinomas, neuroendocrine tumors, and leiomyosarcomas) were also clearly Gb_3-positive. Of note, we have observed a correlation between tumor progression along the adenoma/carcinoma sequence and Gb_3 expression: only malignant lesions expressed high levels of Gb_3, whereas adenomas showed Gb_3 levels that were comparable to normal colon. On a similar note, it had previously been observed that dedifferentiated ovarian carcinomas had high Gb_3 levels, whereas the opposite was observed in differentiated tumors (9). However, and in contrast with other findings for a smaller cohort of tumors (11), we found no significant difference of Gb_3 expression between metastasized and nonmetastasized tumors.

Our observation of Gb_3 expression on human colorectal tumors raises the question of whether Gb_3 expression in tumors represents an overexpression situation or

Published OnlineFirst August 7, 2008; DOI: 10.1158/1535-7163.MCT-08-0430

neoexpression when compared with normal human colonocytes. Several studies showed that human intestinal epithelium (11, 15) and purified epithelial cells (12, 33, 34) were Gb_3-negative. In agreement with these studies, we found that normal human colonocytes were not labeled by STxB, and in our previous *in vivo* experiments on mice, STxB did not accumulate in these cells (30). However, Gb_3 was detectable by lipid extraction on normal colon tissue samples. One source could be stromal cells, such as endothelial and immune cells, or myofibroblasts. Indeed, these cell populations have been reported to express Gb_3 (15, 20, 35). However, it cannot be excluded that some Gb_3 may also be expressed by colonocytes at levels that may be below the threshold for efficient binding of STxB. In this context, it is of interest to indicate that due to the multiligand binding capacity of STxB—up to 15 Gb_3 molecules per pentamer (26)—the binding isotherm of STxB to cells is expected to depend on cellular Gb_3 levels in a complex manner.

Using primary short-term cultures of human tumors, we found that STxB accumulates in the tumors cells of epithelial origin. Uptake was often observed to be increased in tumor cells located at the edges of islets, where prominent lamellipodia were present. This observation may be related to differences in migratory behavior, proliferation state, or cellular differentiation. Indeed, earlier reports found a correlation between cell motility and Gb_3 expression levels in cultured cell lines (11).

STxB remained associated with tumor cells of epithelial origin for several days. We show that this remarkable fact is due to the targeting of STxB into a recently described intracellular transport pathway, the retrograde route (23). Cell counting showed that, on average, >80% of the cells in all primary cultures were STxB-positive, and the majority of cells had internalized the toxin subunit to the Golgi. Moreover, STxB was still present in tumor cells after several days, even though it resided in an as yet ill-defined compartment, reminiscent of observations obtained in the preclinical mouse models (30). This fact may be of great value for the use of STxB for noninvasive tumor imaging because the contrast agents may be cleared from nontumor tissues before image acquisition is started. A possible imaging application of the STxB delivery technology concerns small intestine tumors that cannot be reached by fibroscopy from the stomach or by colonoscopy from the rectum.

We report here that incubation of human primary colorectal tumor cells with fluorescently labeled or unlabeled STxB for various times, and at various concentrations, did not cause apoptosis. Because apoptosis induction by the Shiga toxin receptor Gb_3 has been shown to rely on different mechanisms (33), we used two independent methods for evaluation of cell death: detection of cleaved caspase-3 and detection of cytosolic release of cytochrome *c*.

A recent study reported induction of apoptosis by STxB in colorectal cancer cell lines (11). Another study found no morphologic effect on T84 colon cancer cells after incubation with the holotoxin, but detailed analysis of apoptotic pathways was not done (13). Interestingly, STx2 holotoxin was harmful to intestinal epithelial cells in an organ culture system, even though these cells are Gb_3-negative (13). However, the discussion on apoptosis induction by either Shiga holotoxin or by the B-subunit is controversial. Shiga toxins and verotoxins have been shown to induce apoptosis, resulting in DNA degradation, increase in intracellular Ca^{2+} levels, transitory increase in cyclic AMP levels, and finally, cell lysis (36–40). In fact, STx-induced apoptosis was shown to be accompanied by increased expression of the proapoptotic protein Bax, and inhibited by overexpression of the antiapoptotic protein BCL-2 (37). The relation between the inhibition of protein synthesis by the A-subunit, and the induction of apoptosis is controversial (40–45). In our present study, we used only the nontoxic STxB. It has been shown by several studies that STxB is capable of apoptosis induction in Burkitt's lymphoma cells, although it is not able to inhibit protein synthesis (33, 36, 38).

It is evident from our findings that STxB does not induce apoptosis in primary colorectal cancer cells, the same holds true for epithelial cell lines such as HeLa.[7] Therefore, we believe that cell type–specific differences may be the most likely explanation for the apparent differences in apoptosis induction. This is evident when comparing epithelial cells (such as colorectal cancer cells) to cells of lymphoid origin (such as Burkitt's lymphoma cells). However, differences also undoubtedly exist between the short-term, nonpassaged primary cultures used in this study, and the established colorectal cancer cell lines used in other studies. Cell lines such as T84 or HT29 have been in use for decades and may have therefore acquired genetic and epigenetic alterations not found in the primary tumors. Thus, it seems that apoptosis induction by Shiga toxin strongly depends on the cell type, and may rely on different mechanisms (45).

In order to further elucidate the signaling events that are activated upon ligand binding to the STxB receptor Gb_3 (or CD77) in the primary tumor cells, we used a specific anti-Gb_3/CD77 antibody. The anti-CD77 antibody shares some properties with STxB, but has been shown to trigger different apoptotic pathways in lymphoid cells (33). Incubation with anti-Gb_3/CD77 antibody did not induce activation of caspase-3 in the primary tumor cells. We also observed no induction of caspase-independent apoptosis, as tested by cytosolic release of cytochrome *c*. In contrast, upon treatment with staurosporine, the primary cells from all patients tested underwent rapid and massive apoptosis.

Finally, an important finding of our study is the robust up-regulation of Gb_3 expression by liver metastases and the uptake of STxB by primary cultures from liver metastasis. In colorectal cancer, liver metastases are present in 25% of cases at the time of initial diagnosis, but they caused

[7] Unpublished observations.

Published OnlineFirst August 7, 2008; DOI: 10.1158/1535-7163.MCT-08-0430

the death of a majority of all patients (1). Therefore, early and reliable detection of hepatic colorectal metastasis is of great clinical importance. Gb_3 in metastasis may allow their detection through noninvasive imaging approaches, such as STxB-vectorized positron emission tomography imaging, as described in a previous study on animal models (30). Based on our work, we speculate that the naturally evolved targeting properties of STxB could be diverted for the *in vivo* delivery of contrast agents or therapeutic compounds to colorectal primary carcinomas and metastases.

Disclosure of Potential Conflicts of Interest

No potential conflicts of interest were disclosed.

Acknowledgments

We thank Carmen Marthen for excellent technical assistance; Danijela Vignjevic, Robert Rosenberg, Bernhard Holzmann, and Christophe Rosty are acknowledged for discussion and suggestions.

References

1. Parker SL, Tong T, Bolden S, Wingo PA. Cancer statistics, 1997. CA Cancer J Clin 1997;47:5 – 27.

2. Hakomori S. Traveling for the glycosphingolipid path. Glycoconj J 2000;17:627 – 47.

3. Ono M, Hakomori S. Glycosylation defining cancer cell motility and invasiveness. Glycoconj J 2004;20:71 – 8.

4. Gordon J, Mellstedt H, Aman P, Biberfeld P, Bjorkholm M, Klein G. Phenotypes in chronic B-lymphocytic leukemia probed by monoclonal antibodies and immunoglobulin secretion studies: identification of stages of maturation arrest and the relation to clinical findings. Blood 1983;62: 910 – 7.

5. Murray LJ, Habeshaw JA, Wiels J, Greaves MF. Expression of Burkitt lymphoma-associated antigen (defined by the monoclonal antibody 38.13) on both normal and malignant germinal-centre B cells. Int J Cancer 1985; 36:561 – 5.

6. Oosterwijk E, Kalisiak A, Wakka JC, Scheinberg DA, Old LJ. Monoclonal antibodies against Galα1-4Galβ1-4Glc (Pk, CD77) produced with a synthetic glycoconjugate as immunogen: reactivity with carbohydrates, with fresh frozen human tissues and hematopoietic tumors. Int J Cancer 1991;48:848 – 54.

7. Kalisiak A, Minniti JG, Oosterwijk E, Old LJ, Scheinberg DA. Neutral glycosphingolipid expression in B-cell neoplasms. Int J Cancer 1991;49: 837 – 45.

8. LaCasse EC, Bray MR, Patterson B, et al. Shiga-like toxin-1 receptor on human breast cancer, lymphoma, and myeloma and absence from CD34(+) hematopoietic stem cells: implications for *ex vivo* tumor purging and autologous stem cell transplantation. Blood 1999;94: 2901 – 10.

9. Arab S, Russel E, Chapman WB, Rosen B, Lingwood CA. Expression of the verotoxin receptor glycolipid, globotriaosylceramide, in ovarian hyperplasias. Oncol Res 1997;9:553 – 63.

10. Ohyama C, Fukushi Y, Satoh M, et al. Changes in glycolipid expression in human testicular tumor. Int J Cancer 1990;45:1040 – 4.

11. Kovbasnjuk O, Mourtazina R, Baibakov B, et al. The glycosphingolipid globotriaosylceramide in the metastatic transformation of colon cancer. Proc Natl Acad Sci U S A 2005;102:19087 – 92.

12. Holgersson J, Jovall PA, Breimer ME. Glycosphingolipids of human large intestine: detailed structural characterization with special reference to blood group compounds and bacterial receptor structures. J Biochem (Tokyo) 1991;110:120 – 31.

13. Schuller S, Frankel G, Phillips AD. Interaction of Shiga toxin from *Escherichia coli* with human intestinal epithelial cell lines and explants: Stx2 induces epithelial damage in organ culture. Cell Microbiol 2004;6: 289 – 301.

14. Schuller S, Heuschkel R, Torrente F, Kaper JB, Phillips AD. Shiga toxin binding in normal and inflamed human intestinal mucosa. Microbes Infect 2007;9:35 – 9.

15. Miyamoto Y, Iimura M, Kaper JB, Torres AG, Kagnoff MF. Role of Shiga toxin versus H7 flagellin in enterohaemorrhagic *Escherichia coli* signalling of human colon epithelium *in vivo*. Cell Microbiol 2006; 8:869 – 79.

16. Arab S, Rutka J, Lingwood C. Verotoxin induces apoptosis and the complete, rapid, long-term elimination of human astrocytoma xenografts in nude mice. Oncol Res 1999;11:33 – 9.

17. O'Brien AD, Tesh VL, Donohue-Rolfe A, et al. Shiga toxin: biochemistry, genetics, mode of action, and role in pathogenesis. Curr Top Microbiol Immunol 1992;180:65 – 94.

18. Ling H, Boodhoo A, Hazes B, et al. Structure of the shiga-like toxin I B-pentamer complexed with an analogue of its receptor Gb3. Biochemistry 1998;37:1777 – 88.

19. Katagiri YU, Mori T, Nakajima H, et al. Activation of Src family kinase yes induced by Shiga toxin binding to globotriaosyl ceramide (Gb3/CD77) in low density, detergent-insoluble microdomains. J Biol Chem 1999;274: 35278 – 82.

20. Falguieres T, Mallard F, Baron C, et al. Targeting of Shiga toxin B-subunit to retrograde transport route in association with detergent-resistant membranes. Mol Biol Cell 2001;12:2453 – 68.

21. Mallard F, Antony C, Tenza D, Salamero J, Goud B, Johannes L. Direct pathway from early/recycling endosomes to the Golgi apparatus revealed through the study of shiga toxin B-fragment transport. J Cell Biol 1998;143:973 – 90.

22. Sandvig K, Garred O, Prydz K, Kozlov JV, Hansen SH, van Deurs B. Retrograde transport of endocytosed Shiga toxin to the endoplasmic reticulum. Nature 1992;358:510 – 2.

23. Johannes L, Decaudin D. Protein toxins: intracellular trafficking for targeted therapy. Gene Ther 2005;12:1360 – 8.

24. Johannes L, Tenza D, Antony C, Goud B. Retrograde transport of KDEL-bearing B-fragment of Shiga toxin. J Biol Chem 1997;272: 19554 – 61.

25. Haicheur N, Benchetrit F, Amessou M, et al. The B subunit of Shiga toxin coupled to full-size antigenic protein elicits humoral and cell-mediated immune responses associated with a Th1-dominant polarization. Int Immunol 2003;15:1161 – 71.

26. Bast DJ, Sandhu J, Hozumi N, Barber B, Brunton J. Murine antibody responses to the verotoxin 1 B subunit: demonstration of major histocompatibility complex dependence and an immunodominant epitope involving phenylalanine 30. Infect Immun 1997;65:2978 – 82.

27. Chart H, Law D, Rowe B, Acheson DW. Patients with haemolytic uraemic syndrome caused by *Escherichia coli* O157: absence of antibodies to Vero cytotoxin 1 (VT1) or VT2. J Clin Pathol 1993;46:1053 – 4.

28. Ludwig K, Karmali MA, Sarkim V, et al. Antibody response to Shiga toxins Stx2 and Stx1 in children with enteropathic hemolytic-uremic syndrome. J Clin Microbiol 2001;39:2272 – 9.

29. Levine MM, McEwen J, Losonsky G, et al. Antibodies to shiga holotoxin and to two synthetic peptides of the B subunit in sera of patients with *Shigella dysenteriae* 1 dysentery. J Clin Microbiol 1992; 30:1636 – 41.

30. Janssen KP, Vignjevic D, Boisgard R, et al. *In vivo* tumor targeting using a novel intestinal pathogen-based delivery approach. Cancer Res 2006;66:7230 – 6.

31. Mallard F, Johannes L. Shiga toxin B-subunit as a tool to study retrograde transport. Methods Mol Med 2003;73:209 – 20.

32. Poupon MF, Arvelo F, Goguel AF, et al. Response of small-cell lung cancer xenografts to chemotherapy: multidrug resistance and direct clinical correlates. J Natl Cancer Inst 1993;85:2023 – 9.

33. Tétaud C, Falguières T, Carlier K, et al. Two distinct Gb3/CD77 signaling pathways leading to apoptosis are triggered by anti-Gb3/CD77 mAb and verotoxin-1. J Biol Chem 2003;278:45200 – 8.

34. Bjork S, Breimer ME, Hansson GC, Karlsson KA, Leffler H. Structures of blood group glycosphingolipids of human small intestine. A relation between the expression of fucolipids of epithelial cells and the ABO, Le and Se phenotype of the donor. J Biol Chem 1987;262: 6758 – 65.

35. Obrig TG, Louise CB, Lingwood CA, Boyd B, Barley-Maloney L, Daniel TO. Endothelial heterogeneity in Shiga toxin receptors and responses. J Biol Chem 1993;268:15484 – 8.

Published OnlineFirst August 7, 2008; DOI: 10.1158/1535-7163.MCT-08-0430

36. Gordon J, Challa A, Levens JM, et al. CD40 ligand, Bcl-2, and Bcl-xL spare group I Burkitt lymphoma cells from CD77-directed killing via Verotoxin-1B chain but fail to protect against the holotoxin. Cell Death Differ 2000;7:785 – 94.

37. Jones NL, Islur A, Haq R, et al. *Escherichia coli* Shiga toxins induce apoptosis in epithelial cells that is regulated by the Bcl-2 family. Am J Physiol Gastrointest Liver Physiol 2000;278:G811 – 9.

38. Mangeney M, Lingwood CA, Taga S, Caillou B, Tursz T, Wiels J. Apoptosis induced in Burkitt's lymphoma cells via Gb3/CD77, a glycolipid antigen. Cancer Res 1993;53:5314 – 9.

39. Sandvig K, van Deurs B. Toxin-induced cell lysis: protection by 3-methyladenine and cycloheximide. Exp Cell Res 1992;200:253 – 62.

40. Sandvig K. Shiga toxins. Toxicon 2001;39:1629 – 35.

41. Arab S, Murakami M, Dirks P, et al. Verotoxins inhibit the growth of and induce apoptosis in human astrocytoma cells. J Neurooncol 1998;40:137 – 50.

42. Marcato P, Mulvey G, Armstrong GD. Cloned Shiga toxin 2B subunit induces apoptosis in Ramos Burkitt's lymphoma B cells. Infect Immun 2002;70:1279 – 86 [Retraction in: Marcato P, Mulvey G, Armstrong GD. Infect Immun. 2003;71:4828].

43. Taguchi T, Uchida H, Kiyokawa N, et al. Verotoxins induce apoptosis in human renal tubular epithelium derived cells. Kidney Int 1998;53:1681 – 8.

44. Williams JM, Lea N, Lord JM, Roberts LM, Milford DV, Taylor CM. Comparison of ribosome-inactivating proteins in the induction of apoptosis. Toxicol Lett 1997;91:121 – 7.

45. Cherla RP, Lee SY, Tesh VL. Shiga toxins and apoptosis. FEMS Microbiol Lett 2003;228:159 – 66.

Published OnlineFirst August 7, 2008; DOI: 10.1158/1535-7163.MCT-08-0430

Molecular Cancer Therapeutics

Human colorectal tumors and metastases express Gb_3 and can be targeted by an intestinal pathogen-based delivery tool

Thomas Falguières, Matthias Maak, Claus von Weyhern, et al.

Mol Cancer Ther 2008;7:2498-2508. Published OnlineFirst August 7, 2008.